An Analytical Formulation for Phase Noise in MEMS Oscillators

Deepak K. Agrawal and Ashwin A. Seshia, *Senior Member, IEEE,*

***Abstract*— In recent years, there has been much interest in the design of low noise MEMS oscillators. This paper presents a new analytical formulation for noise in a MEMS oscillator encompassing essential resonator and amplifier nonlinearities. The analytical expression for oscillator noise is derived by solving a second order nonlinear stochastic differential equation. This approach is applied to noise modelling of an electrostatically addressed MEMS resonator-based square wave oscillator in which the resonator and oscillator circuit nonlinearities are integrated into a single modelling framework. By considering the resulting amplitude and phase relations, we derive additional noise terms due to resonator nonlinearities. The phase diffusion of an oscillator is studied, and the phase diffusion coefficient is proposed as a metric for noise optimisation. The proposed nonlinear phase noise model provides analytical insight into the underlying physics and a pathway towards the design optimisation for low noise MEMS oscillators.**

***Index Terms*— MEMS, resonator, oscillator, nonlinear effects, bifurcation, stochastic integration, phase diffusion, amplitude noise, phase noise.**

I. Introduction

Silicon MEMS oscillators have emerged as alternatives to traditional crystal oscillators for a number of applications in timing and frequency control [1]. The advantageous properties of MEMS resonators for these applications include their small size and the potential for tight monolithic or in-package integration with standard CMOS. Recent developments in vacuum packaging [2], temperature compensation [3] and readout electronics [4] have helped to substantially bridge the performance gap with respect to crystal oscillators particularly with regard to long-term stability. However, nonlinear effects are often inherent to the operation of MEMS resonators where power handling is limited by device dimensions and this ultimately places a ceiling on the achievable frequency stability [5].

Noise modelling in MEMS oscillators has always been of interest to the research community as MEMS oscillators continue to be engineered for higher performance applications. However, the current literature on noise modelling in MEMS oscillators is largely based on models developed for standard crystal or electrical oscillators where nonlinear effects are often neglected or not exploited to improve oscillator frequency stability. Moreover, the impact of specific nonlinearities of both the oscillator circuit (e.g. the sustaining amplifier and amplitude limiting mechanism) and the resonator on noise performance have not been considered simultaneously. It should be noted here that previous work by Yurke *et al.* [6] showed that for an oscillator incorporating a Duffing resonator biased at the critical bifurcation point, the contribution of amplifier noise to long-term frequency stability may be suppressed. However, this result was not been pursued substantively through further studies including applications to the MEMS domain until very recent work by Villanueva *et al.* [7] extended this result with an experimental demonstration of noise reduction in a phase-feedback oscillator based on a piezoelectrically driven nonlinear nano-electro-mechanical resonator.

Previous approaches to oscillator phase noise modeling may be broadly classified as linear time invariant (LTI) models, linear time variant (LTV) models and models based on numerical techniques. The LTI models are useful as a starting point but they fail to capture several important effects including the interaction of nonlinearities on noise performance, experimental observations of the up-conversion of low frequency noise and the interaction between amplitude noise and phase noise [8]. These LTI models have been extended using semi-empirical approaches but these approaches do not reveal insight into the underlying physics or enable significant design optimisation studies [5], [9]–[11].

Unlike the LTI approach, LTV models incorporate the time varying nature of an oscillator and can be extended to address the impact of operative nonlinearities in the oscillator loop [12]. However, this approach requires the a-priori knowledge of an Impulse Sensitivity Function (ISF) that is usually obtained only through detailed numerical simulation with analytical formulations available for only the simplest oscillator topologies. Traditional numerical simulators such as SPICE may not integrate nonlinear modelling of the resonator together with circuit nonlinearities. A linear growth of phase fluctuations with respect to the injected noise is an underlying assumption of the LTV approach neglecting the cross-correlation between amplitude and phase fluctuations. Furthermore, both LTI and LTV models calculate an unbounded power spectral density (PSD) at a very small offset from the carrier frequency compared to the typically observed Lorentzian response [12], [13]. Nevertheless, recent attempts have adapted the LTV approach towards the modelling of MEMS oscillators to provide more insight into the impact of nonlinear effects on phase noise with some success [14].

Numerical approaches for oscillator phase noise modeling have made significant progress in recent years. An efficient numerical approach to modeling phase noise in oscillators en-

D. K. Agrawal, Department of Engineering, University of Cambridge, UK. dka23@cam.ac.uk

A. A. Seshia, Department of Engineering, University of Cambridge, UK. aas41@cam.ac.uk

The authors would like to thank the UK-Indian Education and Research Initiative (grant SA06-250) and the Cambridge Trusts for funding support.

compassing non-linearities was proposed by Demir *et al.* [15] and this has since been extended by a number of groups [16], [17] and applied to a diverse range of applications in oscillator noise modeling [18]. The basis of this method is in the application of a nonlinear perturbative analysis about the limit cycle response leading to the calculation of a single scalar quantity representing the variance of the per cycle jitter in the oscillator. The per cycle jitter is dependent not only on the noise generators but also on the calculation of a perturbation projection vector (PPV) and efficient numerical approaches to derive the PPV from the non-linear oscillator dynamics have now been derived [19].

The goal of this paper is to develop an analytical model for oscillator noise which fully considers the essential non-linearities in the resonator and circuit elements comprising the oscillator. As opposed to approaches based on numerical techniques or empirical methods, the analytical expression for phase noise derived in this work enables designer insight into the underlying physics and provides a starting basis for more detailed design optimisation studies. In order to achieve this, we start by integrating the resonator and oscillator circuit nonlinearities into a unified model. This approach enables the investigation of the interaction of these nonlinearities with the injected noise in the oscillator loop.

This paper is organized in six sections. Section II presents a nonlinear electrical model of an electrostatically driven MEMS resonator. Next, nonlinearities in the oscillator circuit are integrated into the model. The description of the oscillator driven by random noise excitation can then be reduced to a second order nonlinear stochastic differential equation (SDE). This modelling approach is applied to a MEMS square-wave oscillator based on electrostatically driven double-ended tuning fork resonator. In Section III, we use the stochastic integration approach to derive analytical expressions for amplitude and phase noise. A comprehensive description of this approach can be found in [20], [21]. In Section IV, the phase noise expression obtained in this work is compared with the established Leeson phase noise model, a nonlinear phase noise model, based on the LTV approach as well as the noise model proposed by Demir *et al.* [15].

The analogy between the random walk of the oscillator phase with the Brownian motion allows for a description of the spectral broadening of the output signal by a phase diffusion process. This leads to a direct correlation between the phase diffusion coefficient and phase noise. Based on this analogy, in Section V, an analysis is carried out to investigate the degree of improvement in phase noise using the diffusion coefficient as a characteristic noise defining parameter. The analysis is then applied to an electrostatically operated double-ended-turning fork (DETF) silicon MEMS square wave oscillator using measured oscillator parameters. Section VI presents a summary and outlook for future work.

II. MEMS Oscillator Model

An oscillator can be conceptually represented by three elements placed in a close loop configuration as shown in Fig. 1. The resonator is a frequency selective element providing a low loss second-order response. This is followed by a gain element, providing for gain and phase conditions to compensate energy dissipation in the loop and ensure that the starting conditions for oscillation are met. Finally, an amplitude limiting mechanism is necessary to regulate oscillation amplitude. This amplitude limited mechanism may be engineered to provide a gain roll-off at large amplitudes or may be inherent to the nonlinearities that are operative in MEMS oscillators. When the oscillator loop gain and phase satisfy the Barkhausen criteria, a steady-state limit cycle behaviour is achieved [22], [23]. In this section, the characteristics of each element are investigated, and consequently an oscillator model is developed.

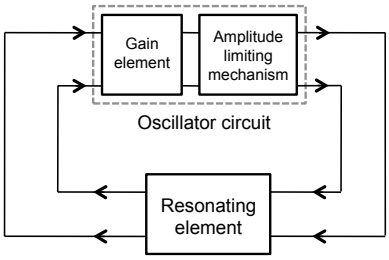

Fig. 1. Block diagram representation of an oscillator.

A. Nonlinear MEMS Resonator Model

To obtain a describing equation of a MEMS oscillator, we start by modelling the nonlinear response of an electrostatically driven micro-resonator. In many instances, the resonator response may be represented by the forced Duffing equation [24]:

$$m\ddot{x} + b\dot{x} + k_o x + k_2 x^3 = f_{ac}(t) \tag{1}$$

where m and b are the lumped effective mass and damping coefficient while k_o and k_2 are the linear and second order spring constants respectively. x is a dynamic displacement variable and $f_{ac}(t)$ is the excitation force. In an electrostatically transduced MEMS resonator, typically k_o is defined by the linear mechanical (k_{om}) and electrical (k_{oe}) spring constants while k_2 represents the cubic nonlinearity of the resonator that combines the mechanical (k_{2m}) and electrical (k_{2e}) second order corrections in the stiffness of the resonator. The mechanical spring constants (k_{om}, k_{2m}) are specific to the topology of the resonator and the selected vibration mode. There are several excellent publications discussing the calculation of k_{2m} for various resonator topologies [5], [25], [26]. The electrical nonlinearities can be determined by calculating the electrostatic force ($F_e(x,t)$) for a given dc bias (V_{dc}) and an ac excitation signal ($v_{\text{ac}}(t)$) applied across the electrodes of the resonator:

$$F_e(x,t) = \frac{1}{2}(V_{\text{dc}} + v_{\text{ac}}(t))^2 \frac{d}{dx} C(x,t) \tag{2}$$

Here, $C(x,t)$ is a time varying dc capacitance which is equal to $\epsilon_o A/(g-x)$ where ϵ_o is the permittivity of air, A is the capacitive area, g is the nominal actuation gap between the driving and sensing electrodes.

Using this expression, the linear electrical spring constant (k_{oe}) and the corresponding first (k_{1e}) and second (k_{2e}) order corrections can be obtained:

$$k_{oe} = -\frac{\epsilon_o A V_{\text{dc}}^2}{g^3},\ k_{1e} = k_{oe}\frac{3}{2g},\ k_{2e} = k_{oe}\frac{2}{g^2} \tag{3}$$

The first order electrical spring constant can be neglected when considering the response at the fundamental frequency. Moreover, as the electrical spring constants are negative, the resonance frequency tends to reduce with higher dc bias. Typically, the mechanical response of the resonator is transduced electrically using a capacitive pick-off scheme.

The parallel-plate capacitive sensing is a well established transduction approach in which a time varying capacitance is formed when a dc bias and ac excitation signal is applied across the actuation gap. The resultant output current can be determined by differentiating the accumulated charge on the parallel-plate capacitor with respect to time:

$$I(t) = \frac{d}{dt}C(x,t)(V_{\text{dc}} + v_{\text{ac}}(t)) \tag{4}$$

In the employed readout mechanism, the output current has two components – the static current and the dynamic current produced due to the static gap between the electrodes and the dynamic motion of the resonator respectively. The magnitude of the dynamic current is increased relative to the static current for $V_{\text{dc}} >> v_{\text{ac}}$. Considering this and using a Taylor series approximation, the output current can be determined from (4) while neglecting the static current term:

$$I = \eta\dot{x}\left(1 + \frac{2x}{g} + \frac{3x^2}{g^2} + O(\varepsilon)\right)_{V_{\text{dc}} >> v_{\text{ac}}(t)} \tag{5}$$

η is a transduction coefficient for parallel-plate electrostatic transducers and is defined as $V_{\text{dc}}\epsilon_o A/g^2$. Moreover, the excitation signal can also be related with the excitation force using η ($f_{ac}(t) = \eta v_{\text{ac}}(t)$). $O(\varepsilon)$ represents the higher order terms which may be neglected when the displacement amplitude is relatively small compared to the actuation gap. To integrate the transduction scheme with (1), we use a describing function approach to simplify (5). Assuming the resonator response is weakly nonlinear and the excitation frequency (ω) is close to the resonance frequency (ω_o), the dynamic displacement may be described as a sinusoidal function $x = x_p \sin\omega t$. Here, x_p is amplitude of the time varying displacement variable. Using the describing function approach, the output current, at ω_o, can be expressed as

$$I(t) \approx \eta\dot{x}\left(1 + \frac{3x_p^2}{4g^2}\right) \tag{6}$$

The electrostatic pull-in in capacitively sensed MEMS resonators limits the maximum obtainable displacement ($g/3$) [27]. Therefore, the maximum error in the output current due to the nonlinear transduction term is less than $\sim$8 % as compared to the linear transduction approximation ($I \approx \eta\dot{x}$). However, in practical cases, the resonators are operated at displacements that are significantly smaller than $g/3$, hence the corresponding error will be correspondingly much smaller than the calculated value. Thus, this analysis assumes a linear transduction relation between the displacement and output current. This allows (1) to be written as

$$\frac{m}{\eta}\dot{I} + \frac{b}{\eta}I + \frac{k_o}{\eta}\int I\,dt + \frac{k_2}{\eta^3}\left(\int I\,dt\right)^3 = \eta v_{\text{ac}}(t) \tag{7}$$

Defining (7) in terms of equivalent circuit parameters:

$$L_m\dot{I} + R_m I + \frac{1}{C_{mo}}\int I\,dt + \frac{k_2}{\eta^4}\left(\int I\,dt\right)^3 = v_{\text{ac}}(t) \tag{8}$$

where

$$L_m = \frac{m}{\eta^2},\ R_m = \frac{\sqrt{k_o m}}{\eta^2 Q},\ C_{mo} = \frac{\eta^2}{k_o} \tag{9}$$

Here, L_m, R_m and C_{mo} are the equivalent motional inductance, resistance and capacitance respectively while Q is the quality factor of the operating vibration mode. Equation (8) describes the nonlinear dynamic response of the resonator in the electrical domain.

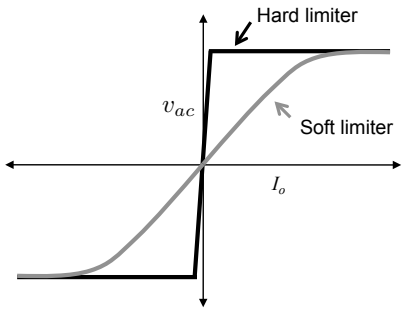

Fig. 2. Qualitative description of a hard and soft limiting mechanisms.

B. Oscillator Circuit Nonlinearities

The differential amplifier based gain element may be mathematically represented by a function describing odd symmetry in the input-output characteristic [28]. In this approximation, the amplifier provides linear gain for small signal input while large signal limiting is approximated by a clipping response. When a purpose-designed amplitude limiting mechanism is employed, the front-end amplifier may be approximated as operating in the linear regime.

The amplitude limiting mechanism can be of either a hard limiting or soft limiting in nature. The hard limiter response saturates at relatively smaller values of the input amplitude while a soft limiter provides a gradual amplitude-dependent gain reduction as illustrated in Fig. 2. By employing a hard limiter between the gain element and the resonator, a square wave oscillator may be developed while a soft limiter is used to implement a sine wave oscillator [29], [30]. In this paper, the analysis is conducted for a MEMS square wave oscillator employing a comparator as the amplitude limiting mechanism. However, this analysis can be readily extended to a MEMS sine wave oscillator as well.

Assuming the response of a hard limiter is symmetrical, a signum function can be used to approximate the response as seen in Fig. 2. To incorporate this response in the model,

we define a function $G(I_o)$, describing the response of a hard limiter at the fundamental frequency [31]:

$$G(I_o) = \frac{V_F}{I_o} \tag{10}$$

Here, I_o is the amplitude of the output current of the resonator while V_F is the constant output amplitude of the hard limiter at the fundamental frequency. In (10), $G(I_o)$ can be considered as a negative resistance as it is a ratio of voltage to current. Now, the characteristics of the hard limiter can be incorporated in the nonlinear electrical mode of the resonator using (8):

$$\begin{aligned} L_m\dot{I} + R_m I - \frac{V_F}{I_o} I + \frac{1}{C_{mo}} \int I\, dt \\ + \frac{k_2}{\eta^4} \left(\int I\, dt \right)^3 = 0 \end{aligned} \tag{11}$$

Note that oscillators do not require an external excitation signal for operation and this is consistent with the formulation in (8).

C. Oscillator Model in Presence of Noise

In an oscillator, various noise sources are operative leading to growing amplitude oscillations when the Barkhausen criteria is met, ultimately converging to steady limit cycle behaviour. The noise sources also result in amplitude and phase fluctuations in the output, as a consequence, the output frequency varies over time. From a modelling perspective, these noise sources can be considered as an equivalent noise voltage (v_n). In this work, it is assumed that v_n is representative of a wide-sense stationary process such as white noise. In this case, (11) can be modified as:

$$\begin{aligned} L_m\dot{I} + R_m I - \frac{V_F}{I_o} I + \frac{1}{C_{mo}} \int I\, dt \\ + \frac{k_2}{\eta^4} \left(\int I\, dt \right)^3 = v_n \end{aligned} \tag{12}$$

If a front-end transresistance amplifier is used as the gain element, (12) can be expressed in terms of output voltage signal $v_a = -R_f I$ where R_f is the feedback resistance of the transresistance amplifier. Further, by using the transformation $v_a = \dot{v}/\omega_o$, the resulting equation can be written as

$$\begin{aligned} \ddot{v} + \frac{R_m}{L_m}\dot{v} - \frac{R_f}{L_m}\frac{V_F}{\rho_o}\dot{v} + \omega_o^2 v + \frac{1}{R_f^2 L_m C_{m2}} v^3 \\ = -\frac{R_f}{L_m}\omega_o v_n \end{aligned} \tag{13}$$

Here, ω_o is the output frequency of the oscillator and is identical to the resonance frequency and may also be expressed as $1/\sqrt{L_m C_{mo}}$. ρ_o is the steady-state output amplitude of a noiseless oscillator. C_{m2} is governed by the cubic nonlinearity of the resonator and defined as

$$C_{m2} = \frac{\eta^4 \omega_o^2}{k_2} \tag{14}$$

It is desirable to eliminate the dependence of (13) on ρ_o as the steady-state output frequency and amplitude are correlated. The solution (13) can approximated as $v = \rho_o \cos\omega_o t$ in the absence of noise. Since we are interested in determining the response near to the fundamental frequency, the following approximation can be used:

$$\text{sgn}(\dot{v}) \approx -\frac{4}{\pi} \sum_{k=0}^{\infty} \frac{\sin(2k+1)\omega_o t}{2k+1} \approx -\frac{4}{\pi} \sin\omega_o t \tag{15}$$

Comparing the derivative of v and (15), leads to

$$\frac{\dot{v}}{\rho_o} \approx \frac{\pi\omega_o}{4} \text{sgn}(\dot{v}) \tag{16}$$

Substituting (16) in (13) and rewriting it in a more compact form:

$$\ddot{v} + \alpha\dot{v} - \beta\text{sgn}(\dot{v}) + \omega_o^2 v + \mu v^3 = -\frac{R_f}{L_m}\omega_o v_n \tag{17}$$

where

$$\alpha = \frac{R_m}{L_m},\ \beta = \frac{R_f}{L_m}\frac{\pi\omega_o V_F}{4},\ \mu = \frac{1}{R_f^2 L_m C_{m2}} \tag{18}$$

Equation (17) is a second order nonlinear SDE. It describes the steady-state response of a MEMS square wave oscillator in the presence of noise. In an independent study, the presented oscillator model in absence of noise has been compared with the experimental data such as output power and frequency for various resonator drive parameters. A good agreement between the between the measured and calculated values is reported [32] providing experimental validation of its applicability.

III. Noise Analysis

The proposed oscillator model equation is solved using nonlinear stochastic analysis to determine the phase noise expression. However, there are other analytical and numerical approaches that may be applied to determine oscillator phase noise in the presence of nonlinearities [15]–[17], [33]–[36].

A. Amplitude and Phase Responses

We start by transforming (17) into a set of equations which describe the amplitude and phase dynamics. We assume the approximate solution of (17) to be

$$v = \rho(t)\cos(\omega_o t + \phi(t)) \tag{19}$$

where $\rho(t)$ and $\phi(t)$ are the time dependent amplitude and phase responses respectively. For simplicity, $\rho(t)$ and $\phi(t)$ are expressed as ρ and ϕ respectively. In the absence of noise, ρ and ϕ are deterministic functions and the spectrum of the oscillator can be represented by two impulse functions at $\pm\omega_o$. However, as mentioned earlier, inherent noise sources in the oscillator results in fluctuations in the amplitude and phase dynamics resulting in spectral broadening about the carrier frequency (ω_o) as inferred from (19). Using the state space method, (17) is converted into two first order differential equations:

$$\dot{z_1} = z_2 \tag{20}$$

$$\dot{z_2} = -\alpha z_2 + \beta\text{sgn}(z_2) - \omega_o^2 z_1 - \mu z_1^3 - \frac{R_f}{L_m}\omega_o v_n \tag{21}$$

where z_1 and z_2 are the state space variables and they are described as $z_1 = v$ and $z_2 = \dot{v}$. In (20) and (21), z_2 is replaced by $-\omega_o y$:

$$\dot{z_1} = -\omega_o y \tag{22}$$

$$\dot{y} = -\alpha y + \frac{\beta}{\omega_o}\text{sgn}(\omega_o y) + \omega_o z_1 + \frac{\mu}{\omega_o} z_1^3 + \frac{R_f}{L_m} v_n \tag{23}$$

Using (19), the state variables can be rewritten in terms of amplitude and phase:

$$z_1 = \rho\cos\theta \tag{24}$$

$$y = \rho\sin\theta \tag{25}$$

Here, the total phase θ is related with the phase drift as $\theta = \omega_o t + \phi$. The first order differential equations of amplitude and phase responses can be obtained from the aforementioned equations. The details of the analysis are shown in Appendix A. The results are

$$\begin{aligned}\dot{\rho} = &-\frac{\alpha\rho}{2}(1-\cos 2\theta) + \frac{\mu\rho^3}{\omega_o}\left(\frac{1}{4}\sin 2\theta + \frac{1}{8}\sin 4\theta\right) \\ &+ \frac{2\beta}{\pi\omega_o}\left(1 - \frac{2}{3}\cos 2\theta - \frac{2}{15}\cos 4\theta\right) \\ &+ \frac{R_f}{L_m} v_n \sin\theta\end{aligned} \tag{26}$$

$$\begin{aligned}\dot{\phi} = &-\frac{\alpha}{2}\sin 2\theta + \frac{\mu\rho^2}{\omega_o}\left(\frac{3}{8} + \frac{1}{2}\cos 2\theta + \frac{1}{8}\cos 4\theta\right) \\ &+ \frac{2\beta}{\rho\pi\omega_o}\left(\frac{4}{3}\sin 2\theta + \frac{8}{15}\sin 4\theta\right) \\ &+ \frac{R_f}{L_m\rho} v_n \cos\theta\end{aligned} \tag{27}$$

Equation (26) and (27) contain rapid oscillation terms ($\omega \geq 2\omega_o$). These high frequency oscillations may be neglected using the conventional "smooth approximation" in which amplitude and phase behaviour are assumed to be slowly-functions of time. This allows averaging out of the high frequency terms over a period of time. Therefore, the approximate modified amplitude ($\dot{\rho}^*$) and phase ($\dot{\phi}^*$) equations can simply be written by neglecting the rapid oscillation terms:

$$\dot{\rho}^* = -\frac{\alpha\rho^*}{2} + \frac{2\beta}{\pi\omega_o} + \frac{R_f}{L_m} v_n \sin\theta^* \tag{28}$$

$$\dot{\phi}^* = \frac{3\mu{\rho^*}^2}{8\omega_o} + \frac{R_f}{L_m\rho} v_n \cos\theta^* \tag{29}$$

In order to determine the fluctuations in amplitude and phase, linearization method is used to obtain simplified equations, by assuming that amplitude of the stochastic terms in the SDE are much smaller than the deterministic terms [37]. Under this assumption, smoothly varying averaged amplitude ($\dot{\rho}_{sm}$) and phase ($\dot{\phi}_{sm}$) responses can be defined by neglecting the noise terms in (28) and (29):

$$\dot{\rho}_{sm} = -\frac{\alpha\rho_{sm}}{2} + \frac{2\beta}{\pi\omega_o} \tag{30}$$

$$\dot{\phi}_{sm} = \frac{3\mu\rho_{sm}^2}{8\omega_o} \tag{31}$$

Now, the fluctuations in amplitude ($\delta\rho$) and phase ($\delta\phi$) may be defined as

$$\delta\rho = \rho^* - \rho_{sm} \tag{32}$$

$$\delta\phi = \phi^* - \phi_{sm} \tag{33}$$

While differentiating (32) and (33), and linearizing them along the smoothly varying trajectories (ρ_{sm}, ϕ_{sm}), the higher orders of $\delta\rho^n$ and $\delta\phi^n$ ($n \geq 2$) are neglected at it is assumed that the deterministic oscillator output dominates over noise. This leads to the simplified equations:

$$\dot{\delta\rho} = -\frac{\alpha}{2}\delta\rho + \frac{R_f}{L_m} v_n \sin\theta_{sm} \tag{34}$$

$$\dot{\delta\phi} = \frac{3\mu\rho_{sm}}{4\omega_o}\delta\rho + \frac{R_f}{L_m\rho_{sm}} v_n \cos\theta_{sm} \tag{35}$$

As (30) describes the smoothly varying averaged output amplitude, it can be shown that ρ_{sm}= ρ_o. Therefore, the approximated steady-state amplitude is determined by equating (30) to zero and using (18):

$$\rho_o = \frac{4\beta}{\pi\omega_o\alpha} = R_f\frac{V_F}{R_m} \tag{36}$$

Using (31) and (36), the modified averaged total phase (θ_{sm}) is given by

$$\theta_{sm} = \omega_1 t + \phi_o \tag{37}$$

where

$$\omega_1 = \omega_o + \frac{3\mu\rho_o^2}{8\omega_o} \tag{38}$$

Here, ω_1 is the modified output frequency, which takes into account the effect of the cubic nonlinearity of the resonator while ϕ_o is the initial phase. Using the steady-state amplitude and phase responses, (34) and (35) can be rewritten as

$$\dot{\delta\rho} = -\frac{\alpha}{2}\delta\rho + \frac{R_f}{L_m}\xi(t) \tag{39}$$

$$\dot{\delta\phi} = \frac{3\mu\rho_o}{4\omega_o}\delta\rho + \frac{R_f}{L_m\rho_o}\zeta(t) \tag{40}$$

Here,

$$\xi(t) = v_n \sin(\omega_1 t + \phi_o) \tag{41}$$

$$\zeta(t) = v_n \cos(\omega_1 t + \phi_o) \tag{42}$$

From (41) and (42), it can be inferred that the contributing noise components in the amplitude and phase fluctuations are orthogonal to each other, thereby, they may be treated as uncorrelated noise sources. Moreover, if the resonator response is linear ($\mu \approx 0$), the amplitude and phase fluctuations are uncorrelated. However, when the resonator is operated in the nonlinear regime, the conventional assumption of equally distributed amplitude and phase noise may not be valid as $\delta\rho$ and $\delta\phi$ are correlated. As v_n is a random variable with flat power spectral density, it can be shown that the autocorrelation of the modulated noise components are [38]

$$\langle\xi(t)\xi(t+\tau)\rangle = \langle\zeta(t)\zeta(t+\tau)\rangle = \frac{\bar{v_n^2}}{4}\delta(\tau) \tag{43}$$

In (43), the correlation is determined at time t and $t+\tau$ where τ represents the variable time shift between the signals.

$\langle\cdot\rangle$ represents the ensemble average of a signal and $\delta(\tau)$ is the Dirac delta function. $\bar{v_n^2}$ is a single-sided power spectral density of the equivalent noise voltage source. It should be noted that this analysis considers noise sources that have equal intensities in the amplitude and phase quadratures. In order to determine the oscillator spectrum, first, the autocorrelation functions of amplitude and phase fluctuations are determined, and then the PSD of the output is calculated.

B. Autocorrelation of Amplitude Fluctuations

Once the steady-state condition is reached, amplitude fluctuations can be determined by applying the Duhamel integration to (39) [39]:

$$\delta\rho(t) = \frac{R_f}{L_m}\int_0^t e^{-\frac{\alpha}{2}(t-t')}\xi(t')\,dt' \tag{44}$$

The autocorrelation function is given by

$$\langle\delta\rho(t)\delta\rho(t+\tau)\rangle = \frac{R_f^2}{L_m^2}\int_0^t\int_0^{t+\tau} e^{-\frac{\alpha}{2}(2t+\tau-t'-t'')} \langle\xi(t')\xi(t'')\rangle\,dt'dt'' \tag{45}$$

Equation (45) can be solved using [20], [21]:

$$\langle\delta\rho\delta\rho_\tau\rangle = \frac{R_f^2}{L_m^2}\frac{\bar{v_n^2}}{4\alpha}e^{-\frac{\alpha}{2}|\tau|} \tag{46}$$

Using (18), rewriting (46) in terms of circuit parameters:

$$\langle\delta\rho\delta\rho_\tau\rangle = \frac{R_f^2}{L_m R_m}\frac{\bar{v_n^2}}{4}e^{-\frac{\alpha}{2}|\tau|} \tag{47}$$

This equation reveals the dependence of the amplitude noise on the gain, provided by the front-end amplifier.

C. Autocorrelation of Phase Fluctuations

Integrating the linearised differential equation of phase fluctuations (40) over a period of time:

$$\delta\phi = \frac{3\mu\rho_o}{4\omega_o}\int_0^t \delta\rho\,dt' + \frac{R_f}{L_m\rho_o}\int_0^t \zeta(t')\,dt' \tag{48}$$

Determining the autocorrelation of (48) as

$$\langle(\delta\phi)^2\rangle = \left(\frac{3\mu\rho_o}{4\omega_o}\right)^2\int_0^t\int_0^t\langle\delta\rho(t')\delta\rho(t'')\rangle\,dt'dt'' + \frac{R_f^2}{L_m^2\rho_o^2}\int_0^t\int_0^t\langle\zeta(t')\zeta(t'')\rangle\,dt'dt'' \tag{49}$$

The solution of this equations is determined using (42), (46) and [38]. The final expression is

$$\langle(\delta\phi)^2\rangle = \left(\frac{3\mu\rho_o}{2\omega_o\alpha}\right)^2\frac{R_f^2}{L_m^2}\frac{\bar{v_n^2}}{4}\left(|t| - \frac{2}{\alpha} + \frac{2}{\alpha}e^{-\frac{\alpha}{2}t}\right) + \frac{R_f^2}{L_m^2\rho_o^2}\frac{\bar{v_n^2}}{4}|t| \tag{50}$$

When $|t| >> 2/\alpha$, (50) may be simplified to

$$\langle(\delta\phi)^2\rangle = \frac{R_f^2}{L_m^2\rho_o^2}\frac{\bar{v_n^2}}{4}\left\{1 + \left(\frac{3\mu\rho_o^2}{2\omega_o\alpha}\right)^2\right\}|t| \tag{51}$$

It is clear from this expression that the phase fluctuations are directly proportional to the integration time when $|t| >> 2/\alpha$. Due to the inherent nature of phase as it neither grows nor decays in a self-sustained oscillator, any perturbations in the phase due to noise get accumulated over time. Consequently, the state point in the phase plane adopts a "random walk" characteristic along the limit cycle [40]. The analogy between the dynamics of the phase perturbation and Brownian motion of unbounded particles enables characterisation of the random walk behaviour as a phase diffusion process. Therefore, (51) can be expressed as

$$\langle(\delta\phi)^2\rangle = D_{\phi_1}|t| \tag{52}$$

where

$$D_{\phi_1} = D_{\phi_o}(1+\gamma^2) \tag{53}$$

$$D_{\phi_o} = \frac{R_f^2}{L_m^2\rho_o^2}\frac{\bar{v_n^2}}{4},\ \gamma = \frac{3\mu\rho_o^2}{2\omega_o\alpha} \tag{54}$$

Here, D_{ϕ_1} and D_{ϕ_o} are considered as nonlinear and linear phase diffusion coefficients respectively. Henceforth, D_{ϕ_1} will be referred to as the diffusion coefficient in this paper. γ is related to the cubic nonlinearity of the MEMS resonator. Rewriting (54) in terms of circuit parameters using (18) and (36):

$$D_{\phi_o} = \frac{R_m^2}{L_m^2V_F^2}\frac{\bar{v_n^2}}{4} \tag{55}$$

$$\gamma = \frac{3V_F^2}{2\omega_o C_{m2}R_m^3} \tag{56}$$

Equation (52) explains the underlying phenomenon by which inherent noise in the oscillator results in perturbations in the phase trajectory. Moreover, it can be inferred that the rate at which state point in the phase plane diffuses is directly proportional to the diffusion coefficient. Therefore, a higher diffusion coefficient may result in larger phase fluctuation. Furthermore, due to the dependence of D_{ϕ_1} on the resonator nonlinearities, a higher phase noise may result when the resonator is driven to larger motional amplitudes.

D. Cross-Correlation between Amplitude and Phase

In order to determine the the oscillator output spectrum, the dependence between the amplitude and phase fluctuations must be calculated when the MEMS resonator is operated in the nonlinear regime. The cross-correlation function can be calculated by multiplying (40) with $\delta\rho$ and then averaging the resulting expression:

$$\langle\delta\rho\delta\phi\rangle = \frac{3\mu\rho_o}{4\omega_o}\int_0^t\langle\delta\rho\delta\rho\rangle\,dt' \tag{57}$$

Using (47), (57) can be simplified:

$$\langle\delta\rho\delta\phi\rangle = \frac{3\mu\rho_o}{4\omega_o}\frac{R_f^2}{L_m^2\alpha^2}\frac{\bar{v_n^2}}{2}(1-e^{-\frac{\alpha}{2}|\tau|}) \tag{58}$$

Rewritten (58) using (18) and (36):

$$\langle\delta\rho\delta\phi\rangle = \frac{3R_f}{4L_mC_{m2}\omega_o}\frac{V_F}{R_m^3}\frac{\bar{v_n^2}}{2}(1-e^{-\frac{\alpha}{2}|\tau|}) \tag{59}$$

From this equation, it can be inferred that the cross-correlation between the amplitude and phase fluctuations is governed by the resonator cubic nonlinearity, feedback signal amplitude and the oscillator loop gain.

E. Spectrum Calculation

The phase noise spectrum is typically calculated from the power spectral density of the oscillator output. In order to determine the output power spectral density, we first calculate the autocorrelation of the output signal v. Consequently, the PSD will be determined by applying the Wiener-Khintchine theorem to the resulting autocorrelation function. The autocorrelation function of (19) is given by

$$\begin{aligned}\langle v(t)v(t+\tau)\rangle = \langle \rho(t)\rho(t+\tau) \\ \cos(\omega_o t+\phi)\cos(\omega_o(t+\tau)+\phi_\tau)\rangle\end{aligned} \tag{60}$$

We define $\rho(t)$ and $\rho(t+\tau)$ as $\rho_o+\delta\rho$ and $\rho_o+\delta\rho_\tau$ respectively. Using these, rewriting (60) as

$$\begin{aligned}\langle vv_\tau\rangle = \frac{1}{2}\mathrm{Re}\Big\{\langle(\rho_o^2+\rho_o\delta\rho+\rho_o\delta\rho_\tau+\delta\rho\delta\rho_\tau)e^{-i\delta\phi}\rangle \\ .e^{-i\omega_o\tau}\Big\}\end{aligned} \tag{61}$$

Assuming the phase fluctuations follow the Gaussian distribution, it can be shown [41]

$$\langle e^{-i\delta\phi}\rangle = e^{-\langle(\delta\phi)^2\rangle/2} \tag{62}$$

Using (62) and [20], (61) can be approximated as

$$\begin{aligned}\langle vv_\tau\rangle = \frac{1}{2}\mathrm{Re}\Big\{(\rho_o^2+\langle\delta\rho\delta\rho_\tau\rangle-(\langle\delta\rho\delta\phi\rangle)^2-2i\rho_o \\ .\langle\delta\rho\delta\phi\rangle)e^{-\langle(\delta\phi)^2\rangle/2}e^{-i\omega_o\tau}\Big\}\end{aligned} \tag{63}$$

Equation (63) has two orthogonal components that contribute to the output spectrum. The first one includes the autocorrelation functions of amplitude and phase fluctuations while the second one is represented by the cross-correlation between amplitude and phase fluctuations due to the cubic nonlinearity of the resonator. Assuming the resonator is operated in a weakly nonlinear regime, using (47) and (59) it can be shown that $\langle\delta\rho\delta\rho_\tau\rangle >> \langle\delta\rho\delta\phi\rangle$. Therefore, (63) may be written as

$$s_{vv}(\tau) = \frac{1}{2}(\rho_o^2+\langle\delta\rho\delta\rho_\tau\rangle)e^{-\langle(\delta\phi)^2\rangle/2}\cos(\omega_o\tau) \tag{64}$$

Substituting (46) and (52) in (64):

$$\begin{aligned}s_{vv}(\tau) = \frac{\rho_o^2}{2}\left\{1+\frac{R_f^2}{L_m^2\rho_o^2}\frac{\bar{v_n^2}}{4\alpha}e^{-\frac{\alpha}{2}|\tau|}\right\} \\ .e^{-\frac{D_{\phi_1}}{2}|\tau|}\cos(\omega_o\tau)\end{aligned} \tag{65}$$

To determine the PSD of $s_{vv}(\tau)$, we apply the Wiener-Khintchine theorem on (65) [42]:

$$S_{vv}(\omega) = \int_{-\infty}^{\infty} s_{vv}(\tau)e^{-i\omega\tau}d\tau \tag{66}$$

While considering $D_{\phi_1} << \alpha$ and using the derived autocorrelation functions of phase and amplitude fluctuations, shown in (51) and (47) respectively, (66) can be simplified to

$$\begin{aligned}S_{vv}(\omega) = \frac{\rho_o^2}{2}\Bigg\{\underbrace{\frac{D_{\phi_1}}{(\omega-\omega_o)^2+D_{\phi_1}^2/4}}_{\text{Phase fluctuation}} \\ +\underbrace{\frac{R_f^2}{L_m^2\rho_o^2}\frac{\bar{v_n^2}}{4}\frac{1}{(\omega-\omega_o)^2+\alpha^2/4}}_{\text{Amplitude fluctuation}}\Bigg\}\end{aligned} \tag{67}$$

In this expression, the resulting output PSD includes components representing the effect of the phase and amplitude fluctuations. This expression can be written in terms of a physical variable such as the output signal at the amplifier using the relation $v_a = \dot{v}/\omega_o$. The expression of a single-sideband PSD of the output is expressed as [43]:

$$\mathcal{L}(\Delta\omega) = 10\log\left(\frac{\omega^2}{\omega_o^2}\frac{S_{vv}}{\rho_o^2/2}\right) \tag{68}$$

By substituting (67) in (68) and using (53), (54), we get

$$\begin{aligned}\mathcal{L}(\Delta\omega) = 10\log\Bigg[\frac{R_f^2}{L_m^2\rho_o^2}\frac{\bar{v_n^2}}{4}\Bigg\{\frac{1+\gamma^2}{\Delta\omega^2+D_{\phi_1}^2/4} \\ +\frac{1}{\Delta\omega^2+\alpha^2/4}\Bigg\}\Bigg]_{\Delta\omega<<\omega_o}\end{aligned} \tag{69}$$

Here, $\Delta\omega$ is the offset from the carrier frequency. This expression includes the spectrum of phase noise and amplitude noise. When the resonator response is linear, γ may be neglected leading to the equal contribution of phase noise and amplitude noise to the output spectrum assuming $\Delta\omega >> D_{\phi_1}/2$ and $\Delta\omega >> \alpha/2$, consistent with the LTI models. However, it can inferred that when γ cannot be neglected, an equal distribution of the output spectrum into phase noise and amplitude noise is no longer valid. As phase noise is the primary metric of significance, the phase noise expression may be expressed in terms of circuit parameters using (18) and (36):

$$\mathcal{L}_\phi(\Delta\omega) = 10\log\left[\frac{R_m^2}{L_m^2V_F^2}\frac{\bar{v_n^2}}{4}\frac{1+\left(\frac{3V_F^2}{2R_m^3\omega_oC_{m2}}\right)^2}{\Delta\omega^2+D_{\phi_1}^2/4}\right] \tag{70}$$

Compared to the existing phase noise models such as [8], [14] which fail to predict bounded phase noise at very small offset with respect to the carrier, (70) predicts the plateau of Lorentzian and flat phase noise response when $\Delta\omega \leq D_{\phi_1}$. Moreover, the expression also reveals the dependence of the phase noise on resonator nonlinearities.

IV. Comparison with existing models

This section compares previous phase noise models with the proposed new model. First, the phase noise expression is rewritten by explicitly adding the noise component (S_n) that exists at the measurement port of an oscillator. By assuming an identical front-end amplifier is used for the measurement port, this contribution can be written as

$$S_n = \frac{\bar{v_n^2}}{v_{sig}^2} \tag{71}$$

Here, v_{sig} is the voltage over the resonator. By adding the injected noise noise component to (70), and using (9), the resulting phase noise expression is:

$$\mathcal{L}_{t\phi}(\Delta\omega) = 10\log\left[S_n\left\{1+\left(\frac{\omega_o}{2Q}\right)^2 \cdot\frac{1+\left(\frac{3V_F^2}{2R_m^3\omega_o C_{m2}}\right)^2}{\Delta\omega^2+D_{\phi_1}^2/4}\right\}\right] \tag{72}$$

This expression for total phase noise will be compared with the existing linear and nonlinear phase noise models.

A. Model comparison - I

The phase noise expression based on a LTI approach can be derived, assuming the approximated output current of the resonator at relatively small offset from the carrier frequency ($\Delta\omega << \omega_o$) to be [44]:

$$I \approx \frac{v_{out}}{R_m + j2\Delta\omega L_m} \tag{73}$$

where v_{out} is the output voltage across the resonator which includes v_{sig} and v_n. Using (9) and $v_{sig} = IR_m$, (73) can be simplified to

$$v_{out}^2 = \bar{v_n^2}\left\{1+\left(\frac{\omega_o}{2Q\Delta\omega^2}\right)^2\right\} \tag{74}$$

Consequently, (74) is normalised with the signal power to determine the phase noise equation:

$$\mathcal{L}_{\phi}(\Delta\omega) = 10\log\left[\frac{\bar{v_n^2}}{v_{sig}^2}\left\{1+\left(\frac{\omega_o}{2Q\Delta\omega^2}\right)^2\right\}\right] \tag{75}$$

This equation is known as the Leeson noise model [13]. It is seen that (72) will lead to a similar expression by making the assumptions that $1/C_{m2} \approx 0$ and $\Delta\omega >> D_{\phi_1}/2$. This model does not address the impact of oscillator nonlinearities on phase noise.

B. Model comparison - II

Recently Ward *et al.* presented a phase noise model addressing nonlinear effects in MEMS resonators [14] which is verified experimentally in an independent study [45]. The model showed that the amplitude-frequency relation adds a new term in the phase noise expression for a LTI model when the MEMS resonator operated in the nonlinear regime. The nonlinear phase noise component is given by

$$S_{\omega n}(\Delta\omega) = \left|\frac{\partial\omega_1}{\partial\rho_o}\right|^2\left|\frac{\partial\rho_o}{\partial V_F}\right|^2\frac{S_{AN}}{\Delta\omega^2} \tag{76}$$

In this expression S_{AN} is the amplitude noise density which is similar to $\bar{v_n^2}$. Using (36) and (38), it can be shown that

$$\frac{\partial\omega_1}{\partial\rho_o} = \frac{3V_F}{4\omega_o R_f R_m L_m C_{m2}} \tag{77}$$

and,

$$\frac{\partial\rho_o}{\partial V_F} = \frac{R_f}{R_m} \tag{78}$$

Substituting (77) and (78) in (76), leads to

$$S_{\omega n}(\Delta\omega) = \left\{\frac{3V_F}{4R_m^2\omega_o L_m C_{m2}}\right\}^2\frac{S_{AN}}{\Delta\omega^2} \tag{79}$$

Equation (79) provides the same additional phase noise component which is obtained in (72) while neglecting D_{ϕ_1} over $\Delta\omega$. Thus, similarities between previous linear and nonlinear models with the proposed nonlinear phase noise expression provide further verification of this approach.

C. Model comparison - III

A general numerical approach to phase noise modeling has been previously presented by Demir *et al.* [15] and further extended by a number of groups [16], [18]. The resulting phase noise expression can be reduced to (Equation (41) in [15])

$$\mathcal{L}_{\phi}(f_m) = 10\log\left(\frac{f_o^2 c}{f_m^2 + \pi^2 f_o^4 c^2}\right) \tag{80}$$

where f_o is the carrier frequency, f_m is the frequency spacing from the carrier and c is a statistical quantity representing the variance in the per cycle jitter. Demir *et al.* and other groups have presented a number of efficient numerical techniques for the calculation of c.

We note that this expression is consistent with the phase noise expression derived in this work. This may be seen by rewriting the phase noise expression using equations (67) and (68) as:

$$\mathcal{L}_{\phi}(\Delta\omega) = 10\log\left(\frac{D_{\phi_1}}{\Delta\omega^2 + D_{\phi_1}^2/4}\right) \tag{81}$$

The following relation between c and D_{ϕ_1} can be inferred by comparing (80) and (81):

$$c = \frac{D_{\phi_1}}{\omega_o^2} \tag{82}$$

Equation (82) is fully consistent with the physical interpretation of the two statistical quantities , D_{ϕ_1} and c, representing the well-established relationship between the variance of the per cycle time jitter and the variance of the per cycle phase jitter of the oscillator [46], [47].

V. Design Trade-off

Next, the phase noise model is employed to find an optimum operating point condition for a MEMS oscillator for improved phase noise response. To provide a realistic framework, a MEMS square wave oscillator is realised on a PCB board and parameters from this oscillator are used for analytical prediction of noise performance [29]. The oscillator consists of an electrostatically driven double-ended-turning fork (DETF) silicon micro-resonator, transimpedance amplifier, bandpass filter and comparator as depicted in Fig. 3(a). The DETF resonator was fabricated in a commercial foundry process using a standard silicon-on-insulator MEMS process (MEMSCAP Inc., USA), and consisted of two clamped-clamped beams and additional moving electrodes. The optical micro-graph of the resonator is shown in Fig. 3(b) while the dimensions

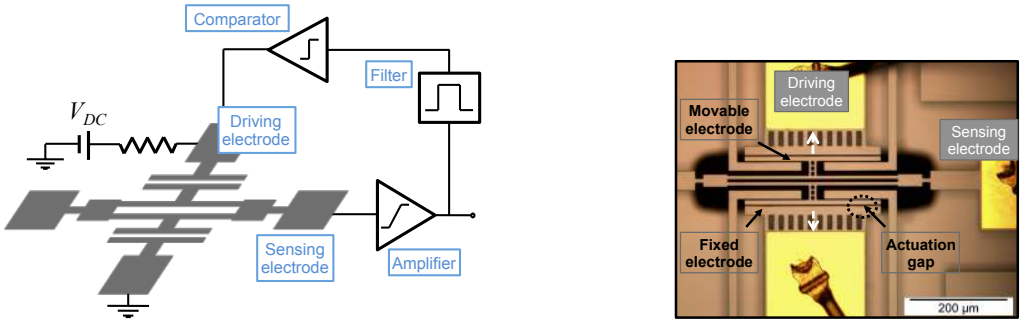

(a) (b)

Fig. 3. (a) Schematic description of the MEMS square wave oscillator. (b) Optical micrograph of the DETF silicon micro-resonator.

are summarised in Table I. The resonator is operated in the primary anti-phase tuning fork flexural mode and capacitive sensing is employed to detect the dynamic motion of the resonator.

TABLE I
DESIGNED DIMENSIONS OF THE DETF SILICON MICRO-RESONATOR.

Parameter	Value (μm)
Beam Length (l_b)	350
Beam width (w_b)	7
Electrode length (l_e)	280
Electrode width (w_e)	10
Device thickness (h)	25
gap (g)	2

The measured open-loop responses at various combinations of dc bias and excitation signal amplitudes are shown in Fig. 4. During measurements, the resonator was placed in a custom vacuum chamber at a pressure of ∼50 mtorr. The extracted parameters from these responses are shown in Table II. Here, the effective mass of the resonator is calculated using [5]:

$$m = 0.375 d_{Si} w_b l_b h + d_{Si} w_e l_e h \tag{83}$$

where d_{Si} is the density of single-crystal silicon.

A. Phase Noise Calculation

Using (72), the phase noise response is calculated for the corresponding feedback signals and dc bias values shown in Fig. 5. In these plots, it is visible that the near-carrier phase noise is significantly impacted by the nonlinear response of the resonator. For operating conditions where the open-loop response of the resonator exhibits multivalued amplitude-frequency behaviour (i.e. bifurcation), higher close-to-carrier phase noise is observed. Therefore, it cannot be concluded that the presence of nonlinearities in the resonator response always degrades or improves the phase noise performance - a turnover point exists as the resonator approaches the nonlinear regime where the noise performance is optimum. This may be observed in Fig. 5(a) and 5(b) where the phase-noise close-to-carrier is lowest when the resonator is operated at 32 mV.

Moreover, based on the calculated values of D_{ϕ_1}, it can be inferred that higher values of the diffusion coefficient result in high near-carrier phase noise as discussed by Ham *et al.* as well [40]. Therefore, diffusion coefficient can be considered as a qualitative parameter to quantify the phase noise in the oscillator. Thus, we refer D_{ϕ_1} as a key metric for further optimisation of phase noise. Now, (53) can be rewriting in terms of oscillator design variables using (55) and (56):

$$D_{\phi_1} = \underbrace{\frac{R_m^2}{L_m^2 V_F^2}\frac{\bar{v_n^2}}{4}}_{\text{Linear component}} + \underbrace{\frac{9V_F^2}{4R_m^4\omega_o^2 L_m^2 C_{m2}^2}\frac{\bar{v_n^2}}{4}}_{\text{Nonlinear component}} \tag{84}$$

From this expression it is clear that the diffusion coefficient demonstrates a dependence on the feedback signal, dc bias and the oscillator loop gain. Moreover, the linear and nonlinear components show different dependence on these parameters. Therefore, design pathways by which the diffusion coefficient may be minimized, resulting in an improved phase noise response are explored. When the resonator is operated at a given dc bias and loop gain, an optimum value of the feedback signal may be found by differentiating (84) with respect to V_F and finding a local minima point. The resulting expression of the optimum feedback signal (V_{Fopt}) is

$$V_{Fopt} = \sqrt{\frac{2}{3} R_m^3 \omega_o C_{m2}} \tag{85}$$

The corresponding diffusion coefficient is calculated by substituting (85) in (84) and using (14) to simplify this further. This leads to the optimum diffusion coefficient ($D_{\phi_1 opt}$):

$$D_{\phi_1 opt} = \frac{3k_2\omega_o}{4k_o^2}\frac{\bar{v_n^2}}{R_m} \tag{86}$$

To validate this expression, a graphical representation of (84) is shown in Fig. 6 at 25 V and 30 V V_{dc}. A local minima can be observed in these plots, which corresponds to a feedback signal amplitude of 24 mV and 30 mV respectively. The corresponding values of the diffusion coefficients are 1.34×10^{-8} sec^{-1} and 1.39×10^{-8} sec^{-1} respectively. While considering Fig. 5, It can be clearly seen that at V_{Fopt}, D_{ϕ_1} attains smaller value, hence validating the expressions (85) and (86). However, as the dc bias is increased from 25 V to 30 V, an increment in D_{ϕ_1} is observed due the reduction in Q factor as shown in Table II.

As can be seen from (86), $D_{\phi_1 opt}$ is proportional to k_2 where $k_2 = k_{2m} + k_{2e}$. In this case, k_{2m} results in spring-hardening and dominates over k_{2e} at high vibration amplitudes

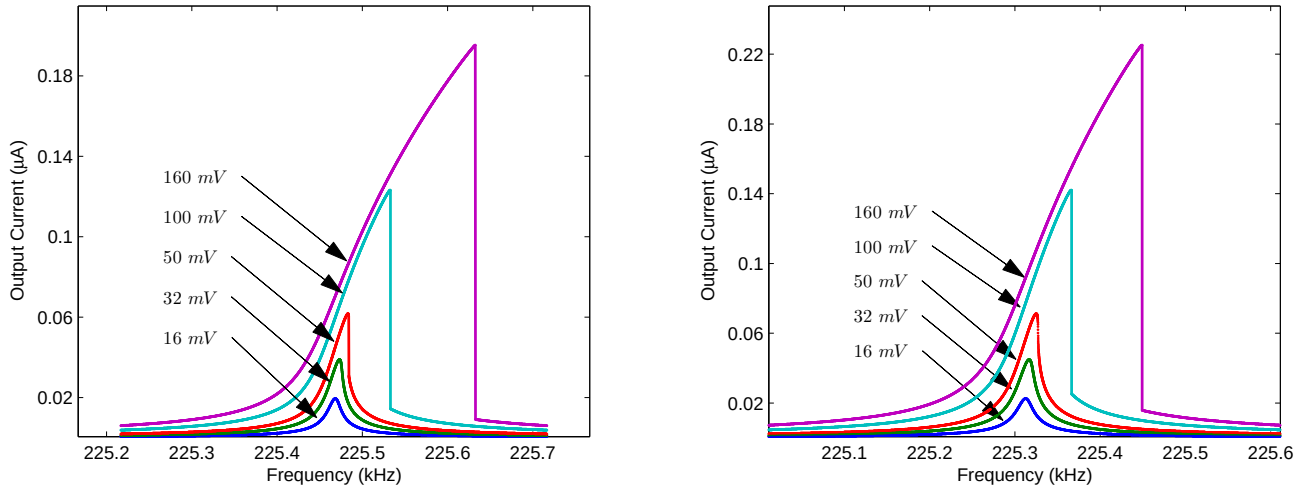

Fig. 4. Measured open-loop response of the electrostatically operated DETF MEMS resonator at a set of v_{ac} and a fixed value of V_{dc} (a) 25 V (b) 30 V. As the excitation signal increases, the amplitude-frequency responses bend towards right due to the mechanical nonlinearities. However, less nonlinear response can be observed with higher dc bias due to the electrical nonlinearities which reduce the overall effect of the cubic nonlinearity.

TABLE II

SUMMARY OF THE EXTRACTED AND CALCULATED PARAMETERS OF THE DETF MEMS RESONATOR.

Parameter	Source	Value at 25 V V_{dc}	Value at 30 V V_{dc}	Unit
m	Equation (83)	2.1710^{-10}	2.1710^{-10}	kg
k_{om}	Measured	436	436	N/m
k_{oe}	Measured	-1.3	-1.9	N/m
k_{2m}	Measured	1.43×10^{12}	1.43×10^{12}	N/m^3
k_{2e}	Measured	-2.7×10^{11}	-3.8×10^{11}	N/m^3
Q	Measured	14588	11674	-
g	Measured	3.1	3.1	μm
V_{dc}	Measured	25	30	V
L_m	Equation (9)	8.4×10^3	5.8×10^3	H
R_m	Equation (9)	8.1×10^5	7×10^5	Ω
C_{mo}	Equation (9)	6×10^{-17}	8.6×10^{-17}	F
C_{m2}	Equation (14)	1.2×10^{-27}	2.7×10^{-27}	FA^2

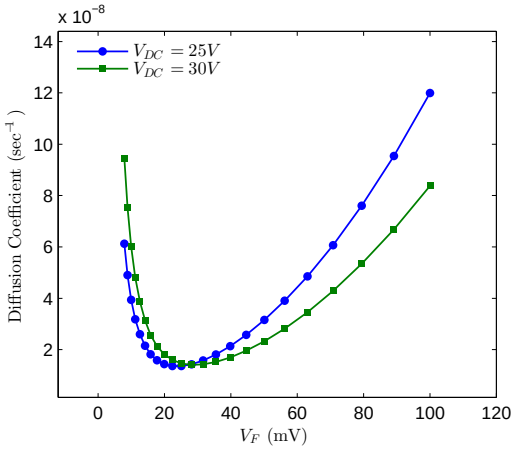

Fig. 6. The effect of the feedback signal on the diffusion coefficient is shown here. It can be clearly seen that D_{ϕ_1} reaches to a minimum value which corresponds to V_{Fopt}

whereas k_{2e} results in spring-softening and may dominate over k_{2m} at high dc voltages and in electrostatically-transduced resonators with small transduction gaps. As the two terms combine with opposite signs, the value of k_2 can be minimized by setting the magnitude of k_{2m} to equal k_{2e}. In systems where mechanical nonlinearities dominate, the reduction of k_2 can be tuned electrically by increasing V_{dc} as can be seen from (3). If the nonlinear component in (84) is neglected, it can be seen that D_{ϕ_1} is inversely related to V_F. For the specific case that k_{2e} is equal to k_{2m}, it is therefore possible to increase output amplitude and simultaneously suppress the increment in the phase diffusion coefficient that would otherwise arise due to the nonlinear term. These findings provide theoretical support to the independent experimental observation of improved phase noise performance for MEMS oscillators wherein the cancellation of the cubic nonlinearity was possible by tuning the electrical stiffness [48]. It is also important to note that the phase diffusion coefficient and the optimum value of V_F is primarily dictated by resonator nonlinearities.

The analysis presented here is applicable to optimization

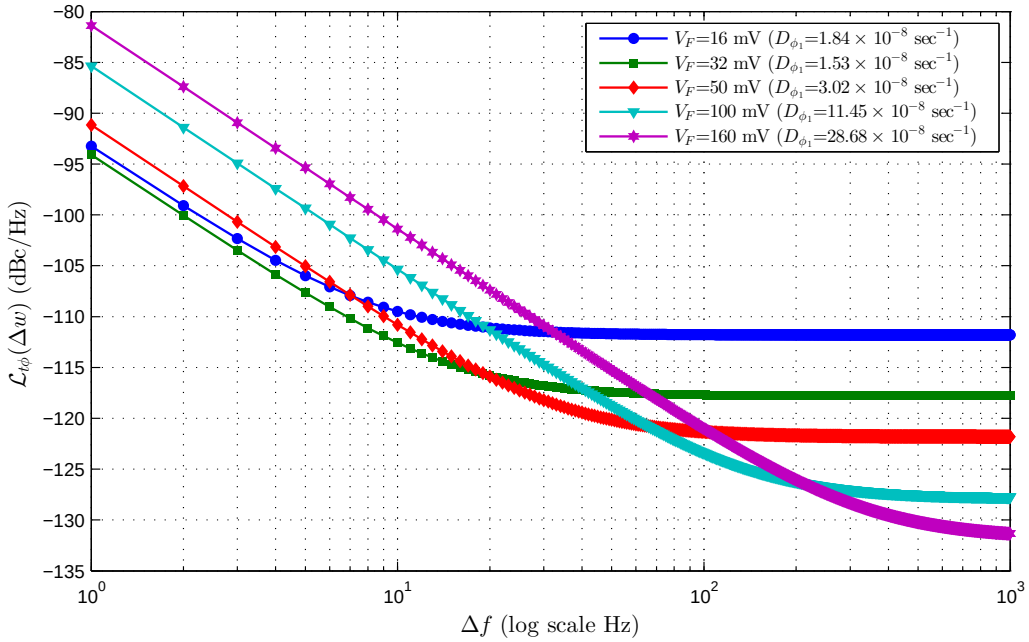

(a)

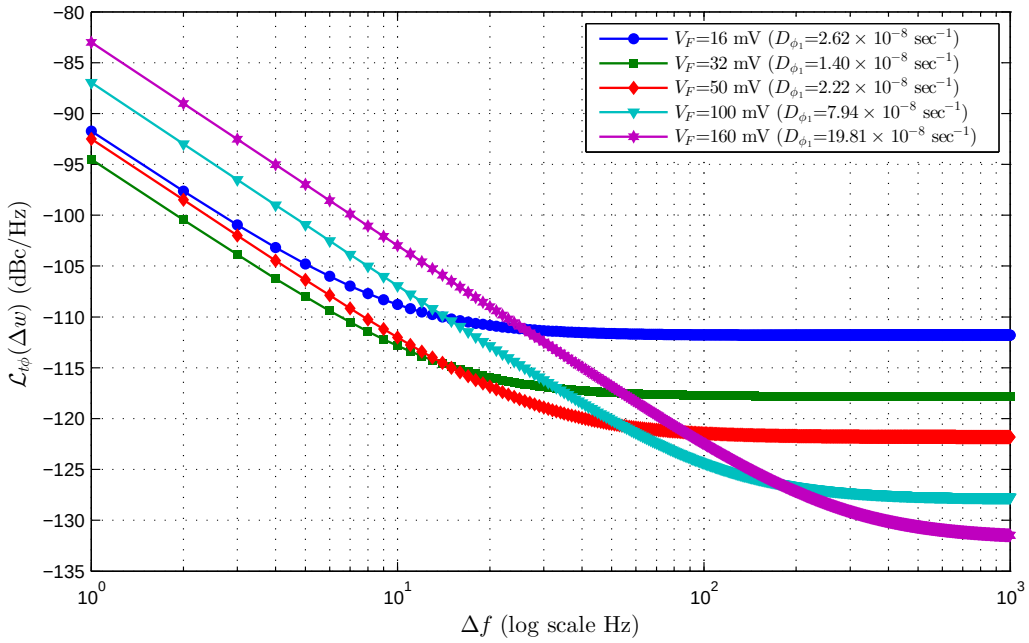

(b)

Fig. 5. Calculated total phase noise plots at a $V_{\rm dc}$ of (a) 25 V (b) 30 V. The phase noise responses are determined at the same values of excitation signals at which the open-loop responses are measured. The calculated values of the diffusion coefficient (D_{ϕ_1}) are also provided.

of the near-carrier phase noise. Equation (72) may now be employed as a starting point for further analysis of noise optimization when MEMS resonators are operated at or near the onset of bifurcation.

VI. Conclusion

Since last decade, there have been several experimental studies to understand the impact of nonlinear effects in MEMS oscillators on the phase noise. In this paper, we presented a new nonlinear phase noise model which adds new insight of understanding the impact of oscillator nonlinearities on the phase noise. By deriving the phase noise expression from a second order nonlinear SDE describing a MEMS square wave oscillator response, we showed how the cubic nonlinearity in a resonator impacts the spectral broadening of the oscillator output. The resulting analytical expression for phase noise is consistent with previously presented non-linear models for oscillator phase noise based on numerical techniques. Moreover, by correlating the simulated phase noise response with parameters obtained from measurements on DETF MEMS resonators, it is demonstrated that the near-carrier phase noise performance may degrade when the resonator is operated beyond the bifurcation point.

The methodology to integrate the resonator and oscillator circuit nonlinearities in a single equation is described for an electrostatically operated MEMS square wave oscillator. However, it can be extended to other MEMS oscillator topologies as well. Moreover, in this work, we only consider the impact of stationary noise in the oscillator. However, the impact of other noise sources and the up-conversion of $1/f$ noise due to nonlinear effects is not considered in this paper. The presented stochastic analysis may however be extended to address the impact of $1/f$ noise.

The presented noise analysis shows the mechanism by which noise in the oscillator is transformed into the phase and amplitude noise. The analytical expression of phase noise is in agreement with existing linear and nonlinear phase noise models. Moreover, we show that the diffusion coefficient which describes the rate of phase diffusion, can be employed as a defining metric for phase noise. By presenting a new analytical framework, this paper provides useful design insight into the noise optimisation for MEMS oscillators. Future work includes the development of a more generalised phase noise model while incorporating other white and non-white noise sources.

Appendix A
Amplitude and phase behaviour

The first derivatives of (23) and (24) are given by

$$\dot{z_1} = \dot{\rho}\cos\theta - \rho\dot{\theta}\sin\theta \tag{87}$$

$$\dot{y} = \dot{\rho}\sin\theta + \rho\dot{\theta}\cos\theta \tag{88}$$

By substituting (23) and (24) in (21) and (22), we get

$$\dot{z_1} = -\omega_o\rho\sin\theta \tag{89}$$

$$\begin{aligned}\dot{y} = -\alpha\rho\sin\theta + \frac{\beta}{\omega_o}\mathrm{sgn}(\omega_o\rho\sin\theta) + \omega_o\rho\cos\theta \\ + \frac{\mu\rho^3}{\omega_o}\cos^3\theta + \frac{R_f}{L_m}v_n\end{aligned} \tag{90}$$

The differential equation of ρ and ϕ can be manipulated from (87)-(90):

$$\begin{aligned}\dot{\rho} = -\alpha\rho\sin^2\theta + \frac{\beta}{\omega_o}\mathrm{sgn}(\omega_o\rho\sin\theta)\sin\theta \\ + \frac{\mu\rho^3}{\omega_o}\cos^3\theta\sin\theta + \frac{R_f}{L_m}v_n\sin\theta\end{aligned} \tag{91}$$

$$\begin{aligned}\dot{\phi} = -\frac{\alpha}{2}\sin 2\theta + \frac{\beta}{\omega_o\rho}\mathrm{sgn}(\omega_o\rho\sin\theta)\cos\theta \\ + \frac{\mu\rho^2}{\omega_o}\cos^4\theta + \frac{R_f}{L_m\rho}v_n\cos\theta\end{aligned} \tag{92}$$

Here, sgn function can be approximated as

$$\mathrm{sgn}(\omega_o\rho\sin\theta) \approx \frac{4}{\pi}\sum_{k=0}^{\infty}\frac{\sin(2k+1)\theta}{2k+1} \tag{93}$$

The amplitude and phase dynamics are determined by replacing (93) in (91) and (92) and taking into account limited rapid oscillation terms. The resulting expressions are

$$\begin{aligned}\dot{\rho} = -\frac{\alpha\rho}{2}(1-\cos 2\theta) + \frac{\mu\rho^3}{\omega_o}\left(\frac{1}{4}\sin 2\theta + \frac{1}{8}\sin 4\theta\right) \\ + \frac{2\beta}{\pi\omega_o}\left(1 - \frac{2}{3}\cos 2\theta - \frac{2}{15}\cos 4\theta\right) \\ + \frac{R_f}{L_m}v_n\sin\theta\end{aligned} \tag{94}$$

$$\begin{aligned}\dot{\phi} = -\frac{\alpha}{2}\sin 2\theta + \frac{\mu\rho^2}{\omega_o}\left(\frac{3}{8} + \frac{1}{2}\cos 2\theta + \frac{1}{8}\cos 4\theta\right) \\ + \frac{2\beta}{\rho\pi\omega_o}\left(\frac{4}{3}\sin 2\theta + \frac{8}{15}\sin 4\theta\right) \\ + \frac{R_f}{L_m\rho}v_n\cos\theta\end{aligned} \tag{95}$$

References

[1] C. T.-C. Nguyen, "MEMS technology for timing and frequency control," *IEEE Transactions on Ultrasonics Ferroelectrics and Frequency Control*, vol. 54, no. 2, pp. 251–270, Feb. 2007.

[2] R. N. Candler, W.-T. Park, H. Li, G. Yama, A. Partridge, M. Lutz, and T. W. Kenny, "Single wafer encapsulation of MEMS devices," *IEEE Transaction on Advanced Packaging*, vol. 26, no. 3, pp. 227–232, Aug. 2003.

[3] S. Pourkamali, G.K. Ho, F. Ayazi, "Low-impedance VHF and UHF capacitive SiBARs. Part I. Concept and fabrication," *IEEE Transactions on Electron Devices*, vol. 54, no. 8, pp. 2017–23, Aug. 2007

[4] G. Langfelder, A. Caspani, and A. Tocchio, "Design criteria of low-power oscillators for consumer-grade MEMS resonant Sensors," *IEEE Transactions on Industrial Electronics*, vol. 61, no. 1, pp. 567–574, Jan. 2013.

[5] V. Kaajakari, T. Mattila, A. Oja, and H. Seppä, "Nonlinear limits for single-crystal silicon microresonators," *Journal of Microelectromechanical Systems*, vol. 13, no. 5, pp. 715–724, Oct. 2004.

[6] B. Yurke, D. S. Greywall, A. N. Pargellis, and P. A. Busch, "Theory of amplifier-noise evasion in an oscillator employing a nonlinear resonator," *Physical Review A*, vol. 51, no. 5, pp. 4211–29, May. 1995.

[7] L. G. Villanueva, E. Kenig, R. B. Karabalin, M. H. Matheny, Ron Lifshitz, M. C. Cross, and M. L. Roukes, "Surpassing fundamental limits of oscillators using nonlinear resonators," *Physical Review Letters*, vol. 110, pp. 177208, Apr. 2013.

[8] S. Lee and C. T. C. Nguyen, "Influence of automatic level control on micromechanical resonator oscillator phase noise," in *Proc. IEEE IFCS*, May 2003, pp. 341–349.

[9] L. He, Y.-P. Xu, and M. Palaniapan, "A state-space phase-noise model for nonlinear mems oscillators employing automatic amplitude control," *IEEE Transactions on Circuits and Systems I-Regular Papers*, vol. 57, no. 1, pp. 189–199, Jan. 2010.

[10] M. Pardo, L. Sorenson, and F. Ayazi, "An empirical phase-noise model for MEMS oscillators operating in nonlinear regime," *IEEE Transactions on Circuits and Systems I-Regular Papers*, vol. 59, no. 5, pp. 979-988, May 2012.

[11] G. Papin, R. Levy, G. Lissorgues, and P. Pouliuchet, "Behavioral modelling of MEMS oscillator and phase noise simulation," *Journal of Analog Integrated Circuits and Signal Processing* vol. 72, no. 1, pp. 11–18, Jul. 2012

[12] A. Hajimiri and T. H. Lee, "A general theory of phase noise in electrical oscillators," *IEEE Journal of Solid-State Circuits*, vol. 33, no. 2, pp. 179–194, Feb. 1998.

[13] D. B. Leeson, "A simple model of feedback oscillator noise spectrum," *Proceedings of the IEEE*, vol. 54, no. 2, pp. 329–330, Feb. 1966.

[14] P. Ward and A. Duwel, "Oscillator phase noise: Systematic construction of an analytical model encompassing nonlinearity," *IEEE Transactions on Ultrasonics Ferroelectrics and Frequency Control*, vol. 58, no. 1, pp. 195–205, Jan. 2012.

[15] A. Demir, A. Mehrotra, and J. Roychowdhury, "Phase noise in oscillators: A unifying theory and numerical methods for characterization," *IEEE Transactions on Circuits and Systems I-Fundamental Theory and Applications*, vol. 47, no. 5, pp. 655–674, May 2000.

[16] F. L. Traversa, F Bonani, "Oscillator noise: a nonlinear perturbative theory including orbital fluctuations and phase-orbital correlation," *IEEE Transactions on Circuits and Systems I-Regular Papers*, vol. 58, no. 10, pp. 2485–97, Mar. 2011.

[17] F. L. Traversa, and F Bonani, "Asymptotic stochastic characterization of phase and amplitude noise in free-running oscillators," *Fluctuation and Noise Letters*, vol. 10, no. 2, pp. 207–221, 2011.

[18] F. Bizzarri, and X. Wei, " Phase noise analysis of a mechanical autonomous impact oscillator with a MEMS resonator," in *Proc. IEEE ECCTD*, Aug. 2011, pp. 729–731.

[19] A. Demir, and J. Roychowdhury, "A reliable and efficient procedure for oscillator PPV computation, with phase noise macromodeling applications," *IEEE Transactions on Computer-Aided Design of Integrated Circuits and Systems*, vol. 22, no. 2, pp. 188–197, Feb. 2003.

[20] R. L. Stratonovich, *Topics in the theory of random noise*. London, U.K.: Gordon and Breach, 1963.

[21] P. I. Kuznetsov, R. L. Stratonovich, and V. I. Tikhonov, *Nonlinear transformations of stochastic processes*. Oxford, U.K: Pergamon, 1965.

[22] E. A. Gerber and A. Ballato, *Precision frequency control, vol. 2, oscillators and standards*. London, U.K.: Academic,, 1985.

[23] R. W. Rhea, *Oscillator design and computer simulation*. London, U.K.: McGraw-Hill, 1997.

[24] D. E. Newland, *Mechanical vibration analysis and computation*. Harlow, U.K.: Longman Scientific & Technical, 1989.

[25] M. I. Younis and A. H. Nayfeh, "A study of the nonlinear response of a resonant microbeam to an electric actuation," *Nonlinear Dynamics*, vol. 31, no. 1, pp. 91–117, Jan. 2003.

[26] V. Kaajakari, T. Mattila, A. Lipsanen, and A. Oja, "Nonlinear mechanical effects in silicon longitudinal mode beam resonators," *Sensors and Actuators a-Physical*, vol. 120, no. 1, pp. 64–70, Apr. 2005.

[27] S. D. Senturia, *Microsystem design*. London, U.K.: Kluwer, 2001.

[28] B. Razavi, *Design of analog CMOS integrated circuits*. London, U.K.: McGraw-Hill, 2001.

[29] J. E. Y. Lee, B. Bahreyni, Y. Zhu, and A. A. Seshia, "A single-crystal-silicon bulk-acoustic-mode microresonator oscillator," *IEEE Electron Device Letters*, vol. 29, no. 7, pp. 701–703, Jul. 2008.

[30] C. T.-C. Nguyen and R. T. Howe, "An integrated CMOS micromechanical resonator high-Q oscillator," *IEEE Journal of Solid-State Circuits*, vol. 34, no. 4, pp. 440–455, Apr. 1999.

[31] P. Grivet and A. Blaquiere, "Nonlinear effects of noise in electronic clocks," *Proceedings of the IEEE*, vol. 51, no. 11, pp. 1606–14, Nov. 1963.

[32] D. K. Agrawal, J. Woodhouse, and A. A. Seshia, "Modeling nonlinearities in MEMS oscillators,"*IEEE Transactions on Ultrasonics Ferroelectrics and Frequency Control*, vol. 60, no. 8, pp. 1646–59, Aug. 2013.

[33] H. Risken and T. Frank, *The Fokker-Planck Equation: methods of solutions and applications*. London, U.K.: Springer, 1989.

[34] M. Lax, "Classical noise. VI. noise in self-sustained oscillators," *Physical Review*, vol. 160, no. 2, pp. 350–366, Feb. 1967.

[35] T. K. Caughey, "Response of van der pol's oscillator to random excitation," *Journal of Applied Mechanics*, vol. 26, no. 3, pp. 345–348, 1959.

[36] F. X. Kaertner, "Analysis of white and $f^{-\alpha}$ noise in oscillators," *International Journal of Circuit Theory and Applications*, vol. 18, no. 5, pp. 485–519, Sep. 1990.

[37] L. Socha, *Linearization Methods for stochastic dynamic systems*. Berlin, Germany: Springer, 2007.

[38] A. Papoulis and S. U. Pillai, *Probability, random variables and stochastic processes*. London, U.K.: McGraw-Hill, 1991.

[39] F. John, *Partial differential equations*. Providence, R.I. : American Mathematical Society, 1998.

[40] D. Ham and A. Hajimiri, "Virtual damping and Einstein relation in oscillators," *IEEE Journal of Solid-State Circuits*, vol. 38, no. 3, pp. 407–418, Mar. 2003.

[41] A. Papoulis, "Random modulation - a review," *IEEE Transactions on Acoustics, Speech and Signal Processing*, vol. 31, no. 1, pp. 96–105, Feb. 1983.

[42] C. Chatfield, *The analysis of time series : An introduction*. London, U.K.: Chapman and Hall, 1980.

[43] E. S. Ferre-Pikal, J. R. Vig, J. C. Camparo, L. S. Cutler, L. Maleki, W. J. Riley, S. R. Stein, C. E. Thomas, F. L. Walls, J. D. White, and D. Joseph, "Draft revision of IEEE std 1139-1988 standard definitions of physical quantities for fundamental frequency and time metrology - random instabilities," in *Proc. IEEE IFCS*, May 1997, pp. 338–357.

[44] V. Kaajakari, J. K. Koskinen, and T. Mattila, "Phase noise in capacitively coupled micromechanical oscillators," *IEEE Transactions on Ultrasonics Ferroelectrics and Frequency Control*, vol. 52, no. 12, pp. 2322–31, Dec. 2005.

[45] H. K. Lee, P. A. Ward, A. E. Duwel, J. C. Salvia, Y. Q. Qu, R. Melamud, S. A. Chandorkar, M. A. Hopcroft, B. Kim, and T. W. Kenny, "Verification of the phase-noise model for MEMS oscillators operating in the nonlinear regime," in *Proc. Transducers*, Jun. 2011, pp. 510–513.

[46] A. Hajimiri, S. Limotyrakis, and T. H. Lee,"Jitter and phase noise in ring oscillators," *IEEE Journal of Solid-State Circuits*, vol. 34, no. 6, pp. 790–804, Jun. 1999.

[47] M. J. Underhill, and P. J. Brown,"Estimation of Total Jitter and Jitter Probability Density Function from the Signal Spectrum," in *IEEE EFTF*, Apr. 2004, pp. 502–508.

[48] M. Agarwal, K. K. Park, R. N. Candler, M. A. Hopcroft, C. M. Jha, R. Melamud, B. Kim, B. Murmann, and T. W. Kenny, "Nonlinearity cancellation in mems resonators for improved power-handling," in *Proc. IEEE IEDM*, Dec. 2005, pp. 295–298.

Deepak Agrawal Biography text here.

Ashwin Seshia Biography text here.